DC Power Flow Feasibility: Positive vs. Negative Loads

Marco Todescato

Abstract— **Voltage instability limits the transmission capacity of a power network. Hence, finding parametric conditions for the feasibility of the power flow equations is of theoretical as well as practical interest. Here, we take over from a recent result tailored for the case of decoupled reactive load flow. For the case of DC power networks, we consider the particular scenario where two different types of loads are present: classical passive loads, modeled as negative quantities, and active loads due to possible distributed generation, modeled as positive quantities. The analysis of the interaction between these two different types of loads leads us to a less conservative estimate of the injection region in parameter space. As a byproduct of the mathematical analysis, we leverage our result into a simple yet numerical exponentially fast algorithm to compute the high-voltage load flow solution. Finally, we extensively verify our findings on standard IEEE test-beds.**

Index Terms— **network transmission capacity, dc power flow analysis, fixed point iterative algorithms**

I. Introduction

Among many different non-linear phenomena characterizing the operational condition of a power system, *voltage instability* and, in particular, voltage collapse, limits the transmission capability of a power network [1]. Indeed, the transmission capacity, i.e., the extent to which a network can deliver power, is constrained by the fundamental physical limits of the network. While approaching this limit, increasingly lower voltages are typically observed, until voltage collapse occurs [2], [3]. Because of the increasing penetration of distributed generation together with the higher and intermittent consumer's demand, today's networks are expected to get dramatically close to their hosting limits. Thus opening unprecedented challenges to systems operators which must guarantee high-quality power delivery to consumers as well as safe operation of the network.

From a purely mathematical perspective, the *Power Flow Equations* (PFEs) model the static interactions and coupling among all the quantities of a power network and their solution space represents all the feasible operating points of the network. Interestingly, since loading-induced voltage collapse can be described statically [4] and thus leveraging static power flow analysis only, by date, voltage collapse studies and characterization of the PFEs solution space are intimately related

Department of Information Engineering, University of Padova, via Gradenigo 6/b, 35131, Padova, Italy. `todescat@dei.unipd.it`.

problems. For instance, along this line of research two sides of the same coin are:

- To synthetize *Voltage Collapse Proximity Indicators* (VCPIs) quantifying margins against collapse.
- To find conditions for the solvability of the PFEs.

VCPIs are typically formulated in voltage-space with the main criticism that, to end up with digestible metrics, relations with the parameter-space are often lost. Conversely, conditions for the solvability of the PFEs are usually formulated in parameter-space. In this case the main criticism relies of the highly non-linear nature of the equations which makes the development of neat analysis extremely hard.

However, despite all the respective pros and cons and the fact that the two topics are often analyzed separately, both classical and current literature can be found. Regarding the synthesis of VCPIs, from the seminal work [5] where is shown that the determinant of the PF Jacobian can be used to measure proximity to collapse, a considerable bunch of literature have been developed considering e.g., eigenvalue [6] and condition numbers indicators [2], continuation methods [7], optimization [8], as well as distributed approaches tailored for distribution networks [9]. Regarding the development of parametric conditions, for the sole case of active power transmission capacity, in [10] the authors present a condition for the synchronization of networks of coupled oscillators in terms of the network parameters. For the reactive decoupled case, in the preliminary work [11] a linear approximation of the load equations is given. Always considering the reactive decoupled case, in the more recent [1] the authors present a sharp parametric condition which guarantees existence, uniqueness and stability of a solution of the power flow equations. Extensions to the active/reactive coupled case with a convenient general linear model for the PFEs can be found in [12], [13].

In this paper, we lean toward developing parametric conditions for the solvability of the PFEs. We consider the case of DC networks. While it is understood that analyzing the coupled AC case is much more appealing from both a theoretical and a practical perspective, it is worth stressing that unraveling the DC case is a necessary condition to promote the development of additional theory. We build our analysis and take over from [1], trying to make a step forward since a disadvantage of the condition in [1] is that it does not distinguish between loads of different nature. Indeed, while traditional loads

are "passive" meaning that they only absorb/consume power (and thus modeled as negative quantities $P < 0$), the penetration of distributed generation foresees the presence of "active" loads. These are able to sustain their own demands while injecting (for some time) additional power back into the grid (thus are modeled as positive $P > 0$). Intuitively, this additional injection positively affects the network loading margin similarly to the well-known principle in AC networks of voltage support by reactive power compensation [14].

The main contributions of the paper are twofold. i) First we present a sufficient condition for the existence of a solution for the DC PFEs. Compared to the condition in [1], its effectiveness is to identify an extended set of solutions when both positive and negative loads are considered. While the results are a preliminary generalization of those in [1] and do not pretend to represent a whole theory on this matter, the ultimate goal is to make a step toward a rigorous understanding of the *interplay* between different types of loads. ii) As second contribution, we present a simple yet (numerical) exponentially fast algorithm to compute the high-voltage solution. The algorithm arises as natural byproduct of a convenient fixed point reformulation of the PFEs.

All the technical proofs are collected in the Appendix.

II. PRELIMINARIES

A. Power Network Model

We model a DC resistive power network as a connected, undirected, weighted graph $(\mathcal{N}, \mathcal{E})$ where $\mathcal{N} = \{1, \ldots, n+m\}$ is the set of nodes (or *buses*) and $\mathcal{E} \subseteq \mathcal{N} \times \mathcal{N}$ is the set of edges (or *branches*) connecting the nodes, that is the set of unordered pairs (i, j), $i, j \in \mathcal{N}$, such that i and j are connected to each other. The edges weights of the graph are given by the electric lines conductances $g_{ij} = 1/r_{ij} > 0$ which we conveniently collect in the conductance matrix $G = G^T$ whose off diagonal elements are given by $G_{ij} = -g_{ij} < 0$, for $(i, j) \in \mathcal{E}$, and diagonal elements $G_{ii} = -\sum_{j \in \mathcal{N}} g_{ij} + g_{s,i}$ with $g_{s,i}$ denoting the node shunt conductance to ground.

Each electric bus $i \in \mathcal{N}$ is described by its nodal voltage to ground $V_i > 0$ and by its power $P_i \in \mathbb{R}$. Hence, the voltage–power relations among buses through branches are given by

$$P_i = \sum_{j \in \mathcal{N}} V_i G_{ij} V_j, \qquad i \in \mathcal{N},$$

which, by collecting voltages and powers in the columns vectors $V, P \in \mathbb{R}^{n+m}$, respectively, can be conveniently rewritten in compact form as

$$P = \mathrm{diag}(V)GV. \tag{1}$$

In the network we consider two types of buses:

1) a set $\mathcal{L} = \{1, \ldots, n\}$ of $n \geq 1$ constant power load buses which are characterized by a constant power P_i while the bus voltage V_i is a free variable.

This type of buses, the most common considered in voltage collapse studies, represents stiff loads whose power level is no voltage dependent. We highlight that the more general ZIP model [15]

$$P_i(V_i) = g_{s,i}V_i^2 + I_{s,i}V_i + P_i. \tag{2}$$

might be considered as well. However, the constant impedance load $b_{h,\text{shunt}}$ can be absorbed in the network shunt conductance; while the constant current portion $I_{s,i}$ can be absorbed into effective generator voltages as shown in [1]. Therefore, without loss of generality we assume a constant power model, i.e., $P_i(V_i) = P_i$.

Observe that this load model is the DC analogous of the well-known *PQ* load model [15] in AC power networks.

2) a set $\mathcal{G} = \{n+1, \ldots, n+m\}$ of $m \geq 1$ generator buses each of them characterized by a constant voltage level $V_i > 0$ acting as a voltage source and where the power demand P_i is a free variable determined by the load power demands.

Observe that this generator model is the DC analogous of the well-known *PV* generator model [3] in AC power networks.

Now, according to the partition of the buses $\mathcal{N}$ into loads $\mathcal{L}$ and generators $\mathcal{G}$, it is convenient to split voltage and power vectors and conductance matrix respectively as

$$V = \begin{bmatrix} V_L \\ V_G \end{bmatrix}, \quad P = \begin{bmatrix} P_L \\ P_G \end{bmatrix}, \quad G = \begin{bmatrix} G_{LL} & G_{LG} \\ G_{GL} & G_{GG} \end{bmatrix}.$$

Accordingly, the power flow Eq. (1) can be rewritten as

$$P_L = \mathrm{diag}(V_L)(G_{LL}V_L + G_{LG}V_G), \tag{3a}$$

$$P_G = \mathrm{diag}(V_G)(G_{GL}V_L + G_{GG}V_G). \tag{3b}$$

Observe that, since the generator voltages V_G are given and fixed, upon solving Eq. (3a) for V_L, Eq. (3b) can be trivially solved to compute the generator powers P_G.

For the matrix G_{LL}, which we refer to as *grounded conductance matrix*, we assume the following

Assumption 2.1 (Properties of G_{LL}): The matrix G_{LL}:

1) is a non-singular positive symmetric M-matrix[1];
2) the graph associated to it, that is the graph associated to the load nodes, is connected.

The first of Assumptions 2.1 is always verified in practice [16] and always satisfied in the absence of line-charging and shunt capacitors. The second assumption can be made without loss of generality, see [1, Supplementary Info]. Thanks to Assumption 2.1, G_{LL} is invertible and G_{LL}^{-1} is a dense matrix with positive elements. It is then convenient to define the *open-circuit* voltage profile [1]

$$V_L^* := -G_{LL}^{-1}G_{LG}V_G > 0 \ \in \mathbb{R}^n. \tag{4}$$

---

[1]An M-matrix A is a matrix with negative off-diagonal elements and positive diagonal ones which can be expressed in the form $A = sI - B$, with $b_{ij} \geq 0$, $s > \rho(B)$, the maximum of the moduli of the eigenvalues of B and I is the identity matrix.

This represents the high-voltage solution of (3a) when all the loads are open-circuited, i.e., $P_L = \mathbb{0}_n$. Note that, thanks to properties of G_{LL}, $V_L^* > 0$. Thanks to (4), Eq. (3a) can be further simplified as

$$P_L = \mathrm{diag}(V_L)G_{LL}(V_L - V_L^*).\tag{5}$$

B. Loading Margin for DC Networks

Here, we review the main result of [1], which we refer the reader to for all the technical details.

The final goal of [1] was to identify a suitable loading margin for decoupled networks concisely expressed in parameter-space rather than as (generally) complicated functions in voltage-space, e.g., determinant of the PFEs Jacobian, eigenvalue, singular value or condition number computations.

To this aim, denoting with $\delta \in [0,1)$ the percentage deviation of a load voltage V_i, $i \in \mathcal{L}$, from the corresponding open-circuit solution V_i^*, it is possible to define the *security set*

$$\overline{\mathcal{S}}(\delta) := \{V_L \in \mathbb{R}_{\geq 0}^n : (1-\delta)V_L^* \leq V_L \leq (1+\delta)V_L^*\},\tag{6}$$

with interior $\mathcal{S}(\delta)$ and where the inequalities are defined element-wise. In [1] the authors were interested in characterizing the solutions $V_L \in \overline{\mathcal{S}}(\delta)$. To quantify the strength of the network, define the *critical load matrix* $P_{\mathrm{crit}} \in \mathbb{R}^{n \times n}$ as

$$P_{\mathrm{crit}} := \frac{1}{4}\mathrm{diag}(V_L^*)G_{LL}\mathrm{diag}(V_L^*)\tag{7}$$

which, from Assumption 2.1 and the fact that $V_L^* > \mathbb{0}_{n_\ell}$, is a positive definite M-matrix. Then, Theorem 1 in [1] gives a sufficient parametric condition for the existence and uniqueness of a high-voltage solution for the decoupled PFEs (5) which states that if

$$\Delta := \|P_{\mathrm{crit}}^{-1}P_L\|_\infty < 1$$

then $\exists! \; V_L \in \overline{\mathcal{S}}(\delta_-)$ where $\delta_- \in [0, \frac{1}{2}[$ is one of the two solution of the equation $4\delta(1-\delta) = 0$.

The condition above is extremely concise and represents a voltage collapse proximity indicator directly in parameter space. Yet, a conservative aspect is that it does not distinguish between passive and active loads, i.e., between loads than simply absorb/consume power versus loads that might be equipped with distributed generation to injected/provide power. Thus, in the following we try to explicitly take into account the interplay between the two different types of loads.

III. Enhanced Loading Margin

We are interested in capturing the interplay between *injected* (modeled as $P > 0$) and *consumed* (modeled as $P < 0$) power at load buses and its effect on the network loading margin. Intuitively, the presence of active buses, able to sustain their own load while providing additional power, should be beneficial from a loading margin perspective. For the case of AC networks, this can be viewed as the conventional power engineering

practice analogue of supporting the voltages by reactive power compensation [14].

First of all, it is convenient to separate "active" buses where power is injected, denoted with $P_L^+ \in \mathbb{R}^n$, from those where power is consumed, denoted with $P_L^- \in \mathbb{R}^n$. These are element-wise defined, for $i \in \mathcal{L}$, as

$$[P_L^+]_i := \begin{cases} [P_L]_i & \text{if } [P_L]_i > 0, \\ 0 & \text{otherwise.} \end{cases}$$
$$[P_L^-]_i := \begin{cases} -[P_L]_i & \text{if } [P_L]_i < 0, \\ 0 & \text{otherwise.} \end{cases}\tag{8}$$

In the the following, given a vector $x \in \mathbb{R}^n$, $\|x\|_{+\infty}$ denotes the standard $\infty-$norm while, with a slight abuse of notation, we define $\|x\|_{-\infty} := \min_h |x_h|$, which is not a proper norm. In addition, we define the following real quantities:

$$\begin{aligned}\varphi_+ &:= \|P_{\mathrm{crit}}^{-1}P_L^+\|_{+\infty} - \|P_{\mathrm{crit}}^{-1}P_L^-\|_{-\infty}, \\ \Phi_+ &:= \|P_{\mathrm{crit}}^{-1}P_L^+\|_{+\infty} + \|P_{\mathrm{crit}}^{-1}P_L^-\|_{-\infty}, \\ \varphi_- &:= \|P_{\mathrm{crit}}^{-1}P_L^+\|_{-\infty} - \|P_{\mathrm{crit}}^{-1}P_L^-\|_{+\infty}, \\ \Phi_- &:= \|P_{\mathrm{crit}}^{-1}P_L^+\|_{-\infty} + \|P_{\mathrm{crit}}^{-1}P_L^-\|_{+\infty}.\end{aligned}\tag{9}$$

We now present our main result consisting in a sufficient condition for the existence of a solution $V_L \in \mathbb{R}_{\geq 0}^n$ of (5).

Theorem 3.1 (Enhanced Feasibility Condition): Consider the PFEs (5). Define V_L^* as in (4), P_{crit} as in (7), and the active and passive load vectors P_L^+ and P_L^- as in (8). Compute δ_- and δ_- as the output of Algorithm 1. Then, if $\delta_- \leq \delta_+$:

1) **Secure Solution:** There exists at least one solution $V_L \in \overline{\mathcal{S}}(\delta_-)$ of the DC PFEs (5);
2) **Solutionless Region:** There exists no solutions of the DC PFEs (5) in the open set

$$\{V_L \in \mathbb{R}^{n_\ell} : V_L > (1 - \delta_+)V_L^* \text{ and } V_L \notin \overline{\mathcal{S}}(\delta_-)\}.$$

Remark 3.2 (Computational aspects): As outlined in Algorithm 1, the parameters δ_-^{up}, δ_+^{up}, δ_-^{low} and δ_+^{low} are the solutions of a third order equations. To explicitly compute their values is possible either to exploit a numerical approach, e.g., a Newton-Raphson algorithm, or to use the closed form expression. $\qquad\square$

Observe that, Algorithm 1 might not found admissible solutions for the upper and lower inequalities. Obviously, if this is the case, the statement of Theorem 3.1 cannot be checked and nothing can be said on the solvability of the PFEs (5). Despite that, the conditions of both Theorem 1 in [1] and Theorem 3.1 can be interpreted as providing estimates of the injection region of the power network, i.e., the set of power demands in load-space for which at least one high-voltage solution exists. These estimates, of which a numerical comparison for a simple two-load case system is reported in Section IV-A, are implicit in the respective conditions. Namely, if the conditions are satisfied for a set of injections P_L, then P_L is in the injection region. Since Theorem 3.1

Algorithm 1 Enhanced Sufficient Feasibility Condition

Require: Φ_+, φ_+, Φ_-, φ_-. **Define:**

$$y_{\mathrm{up}}(\delta) := \varphi_+ + \Phi_+\delta \,,$$
$$y_{\mathrm{low}}(\delta) := \varphi_- - \Phi_-\delta \,,$$
$$g(\delta) := 4\delta(1 - \delta^2) \,.$$

1: {Upper Bound Check:}
2: **if** $0 \le \varphi_+ \le 1$ **and** $\Phi_+ \le 4 - 12\left(\frac{\varphi_+}{8}\right)^{\frac{2}{3}}$ **then**
3:   compute $\delta_-^{\mathrm{up}} \in [0, \frac{1}{2}]$ and $\delta_+^{\mathrm{up}} \in [\frac{1}{2}, 1]$ as the unique solutions of the third order equation $y_{\mathrm{up}}(\delta) = g(\delta)$
4: **else if** $\varphi_+ < 0$ **then**
5:   set $\delta_-^{\mathrm{up}} := 0$ and compute δ_+^{up} as

$$\delta_-^{\mathrm{up}} := \min\{y_{\mathrm{up}}(\delta) = g(\delta)\,,\ 1\}$$

6: **end if**
7:
8: {Lower Bound Check:}
9: **if** $-1 \le \varphi_- \le 0$ **and** $\Phi_- \le 4 - 12\left(-\frac{\varphi_-}{8}\right)^{\frac{2}{3}}$ **then**
10:   compute $\delta_-^{\mathrm{low}} \in [0, \frac{1}{2}]$ and $\delta_+^{\mathrm{low}} \in [\frac{1}{2}, 1]$ as the unique solutions of the third order equation $y_{\mathrm{low}}(\delta) = -g(\delta)$
11: **else if** $\varphi_- > 0$ **then**
12:   set $\delta_-^{\mathrm{low}} := 0$ and compute δ_+^{low} as

$$\delta_+^{\mathrm{low}} := \min\{y_{\mathrm{low}}(\delta) = -g(\delta)\,,\ 1\}$$

13: **end if**
14:
15: **if** Admissible solutions have been found **then**
16:   $\delta_- := \max\{\delta_-^{\mathrm{low}}, \delta_-^{\mathrm{up}}\}\,,\quad \delta_+ := \min\{\delta_+^{\mathrm{low}}, \delta_+^{\mathrm{up}}\}\,.$
17: **else**
18:   Return -1 (no solution found)
19: **end if**

---

generalizes Theorem 1 in [1] the following corollary is straightforward.

Corollary 3.3 (Injection Region of DC PFEs): The estimated injection region for the DC PFEs (5) identified by the conditions of Theorem 3.1 is greater than or equal to that identified by Theorem 1 in [1]. $\square$

In view of Corollary 3.3, it is easy to see that when only one type of load is present then Theorem 3.1 collapses onto Theorem 1 in [1].

Remark 3.4 (Geometrical Intuition): From a strictly mathematical point of view, the parameters of Eq. (9) represents slopes, Φ, and intercepts, φ, of some lines whose relative geometrical positions, under the conditions of Theorem 3.1, identify an invariant set for an appropriate fixed point mapping (see Appendix). $\square$

Remark 3.5 (Physical Intuition on $P_{\mathrm{crit}}^{-1}P_L^+$, $P_{\mathrm{crit}}^{-1}P_L^-$): Consider the PFEs (5), and define the normalized voltage profile $v := \mathrm{diag}(V_L^*)^{-1}V_L$, well defined since $V_L^* > 0$. Exploiting P_{crit} in (7), Eq. (5) can be rewritten

as

$$P_L = 4\,\mathrm{diag}(v)P_{\mathrm{crit}}(v - \mathbb{1})\,, \qquad (10)$$

and for lightly loaded networks, i.e., $\|P_L\| \sim 0$, it is expected that $V_L \simeq V_L^*$, i.e., $v \simeq \mathbb{1}$. Then, to first order, the solution of (10) is given by

$$v \simeq \mathbb{1} + \frac{1}{4}P_{\mathrm{crit}}^{-1}P_L = \mathbb{1} + \frac{1}{4}(P_{\mathrm{crit}}^{-1}P_L^+ - P_{\mathrm{crit}}^{-1}P_L^-) \quad (11)$$

From (11), the first-order solution consists of a uniform profile $\mathbb{1}$, plus a deviation which depends on the loading condition, with the matrix P_{crit}^{-1} providing the conversion between load-space and voltage-space. In particular, since P_{crit}^{-1} is a dense positive matrix, $P_{\mathrm{crit}}^{-1}P_L^+$ provides voltage support while $P_{\mathrm{crit}}^{-1}P_L^-$ makes the voltage to drop. One can observe that the parameters φ_+ and φ_- are the difference between the maximum positive and the minimum negative deviations, and the minimum positive and the maximum negative deviations, respectively. To this extent, the parameters represent the maximum possible positive and negative linear deviation from the open-circuit solution V_L^*. $\square$

A. Solving the PFEs - An exponentially fast algorithm

The condition of Theorem 3.1 can be effectively used for monitoring and security purposes. Besides that however, if solutions exist, it is convenient to be able to compute at least one of them. Here, we present a simple yet (numerically) exponentially fast algorithm to compute one solution of (5). The algorithm naturally arises from a convenient fixed point reformulation of (5). Indeed, defining the *deviation* vector of V_L from the open-circuit profile V_L^* as $x := \mathrm{diag}(V_L^*)^{-1}V_L - \mathbb{1} \in \mathbb{R}^n$, Eq. (5) can be rewritten as

$$x = f(x) := -\frac{1}{4}P_{\mathrm{crit}}^{-1}\mathrm{diag}(P_{\mathrm{L}})r(x) \qquad (12)$$

where $r(x) = \left[\frac{1}{1+x_1}, \dots, \frac{1}{1+x_n}\right]^T$. The *Fixed Point* (FP) Algorithm 2 shows how to leverage (12), which can be regarded as an algorithmic iteration of an iterative algorithm, to compute one solution of the PFEs (5).

Algorithm 2 Fixed Point (FP)

Require: $P_{\mathrm{crit}}^{-1}\mathrm{diag}(P_{\mathrm{L}})$, $x(0) = 0$, $\epsilon > 0$
1: **repeat**
2:   $x(k+1) = f(x(k)) = -\frac{1}{4}P_{\mathrm{crit}}^{-1}\mathrm{diag}(P_{\mathrm{L}})r(x(k))$
3: **until** $\|x(k+1) - x(k)\| < \epsilon$

Remark 3.6 (Stopping Criterion): In Algorithm 2, ϵ is a user-defined parameter which sets the stopping criterion and, in turn, the convergence accuracy.

IV. SIMULATION RESULTS

Here we test the condition of Theorem 3.1 as well as the proposed FP Algorithm 2. All the simulations are run in Matlab on a 2.53GHz Intel Core 2 Duo processor with 8GB of RAM. The standard power flow solver used is Matpower [17].
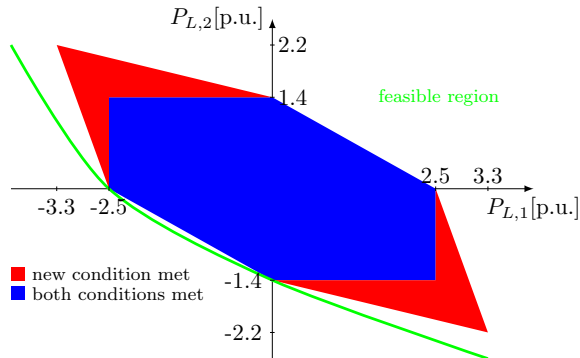
Fig. 1: Plot, in the load space, of the feasible loading configurations. The green line denotes the limit of the feasible region. The blue area identifies loading conditions satisfying both the new proposed condition and the condition in [1]. The red areas identify conditions where only the new condition is met.

A. Three-nodes case study

For a three buses network which represents the minimum working example to have both active/positive and passive/negative loads, it is possible to explicitly plot the solutions of the PFEs in load space. For each solution, we can check the condition of Theorem 3.1 against the one in [1]. We consider a simple network with line topology – generator-load-load – with electric lines with conductances equal to 10[p.u.] and 14[p.u.], respectively. Load demands are expressed in [p.u.] values. Figure 1 shows in green the limit of the feasible region, i.e., the region where solutions of the PFEs can be found. The blue area represents loading configurations captured by both Theorem 3.1 and the condition in [1]. Finally, the red areas represent those configurations where only the new condition is met. As can be seen, the feasible region grows in the positive orthant direction, which correspond to positive/injected loads, but none of the two conditions is able to capture it. Moreover, as expected, in the case of single-type loads, either positive or negative, the proposed condition collapses onto the one in [1]. The more interesting case of mixed loads shows that the new feasibility condition better captures the network capacity.

B. Test on standard IEEE transmission networks

Here we perform tests on a set of standard transmission networks tranformed into DC equivalent by considering just the resistive part. Specifically, for each network we perform a Monte Carlo simulation over 1000 runs where at each run we randomize 100% of the demand and check i) if a solution is found, ii) if the proposed condition is satisfied and iii) if the condition of [1] is verified. Table I reports the results. Note that, even if the improvement from the condition in [1] is not considerable, the new condition is able to capture, in all the cases, a bigger set of feasible loading configurations.

Grid	9 bus	14 bus	30 bus	39 bus
# Loads	6	9	24	29
# Generators	3	5	6	10
Solution Found	49.90%	91.20%	76.30%	55.70%
$\Delta < 1$	18.50%	79.80%	27.50%	10.00%
New Condition Met	19.40%	80.30%	29.20%	11.60%

TABLE I: Results for different IEEE standard grids averaged over 1000 Monte Carlo runs.
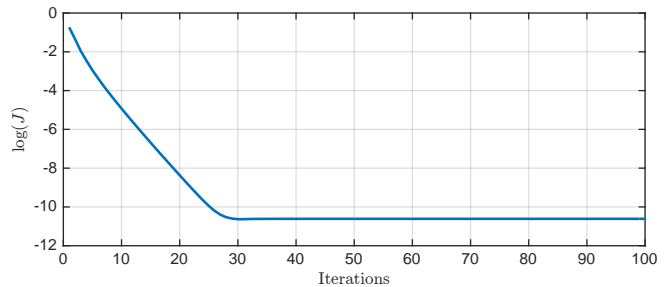
Fig. 2: Numerical average convergence rate of the FP algorithm.

C. FP algorithm

Here, we show the effectiveness of the proposed FP Algorithm 2.

First, we show the (numerical) exponential convergent behavior of the FP algorithm. The test-bed considered is the IEEE 30 bus transmission grid. We compare the solution of our FP algorithm with the solution previously computed thanks to the standard Matpower solver. Figure 2 shows, in logarithmic scale, the average over 1000 Monte Carlo successful realizations, of

$$J := \|V_{L,\mathrm{FP}} - V_{L,\mathrm{MP}}\|_\infty \,,$$

where the subscripts "FP" and "MP" stand for *Fixed Point* and *Matpower*, respectively.

As second comparison, we test the FP algorithm in terms of execution time against the Fast Decoupled Power Flow Matpower solver over different IEEE transmission grids. A set of Monte-Carlo samples have been uniformly drawn randomizing 100% of the demand. The power flow equations have been solved with the standard Matpower solver and with a modified solver where the standard Matpower's Newton-Raphson iteration to compute the step to update the voltage magnitudes is substituted by the FP algorithm. We consider 1000 successful realizations, where both the standard and the modified solvers converge. Table II shows comparable performance. Yet, the modified solver behaves slightly better. In flavor of Table II, for the 118 bus system only, Figure 3 plots the execution times of 25 different runs for both the standard MP solver and the modified one, denoted as FP. As can be seen the average running time (dashed horizontal lines) corresponding to the FP solver is lower than that of the standard MP solver. Finally, we compare the standard Fast Decoupled Power Flow

Grid	9 bus	14 bus	39 bus	57 bus	118 bus
MP	11.0	10.4	12.0	12.2	13.4
FP	9.7	9.2	10.3	10.8	10.8

TABLE II: Average execution time in [ms] over 1000 Monte Carlo runs for different standard transmission grids.
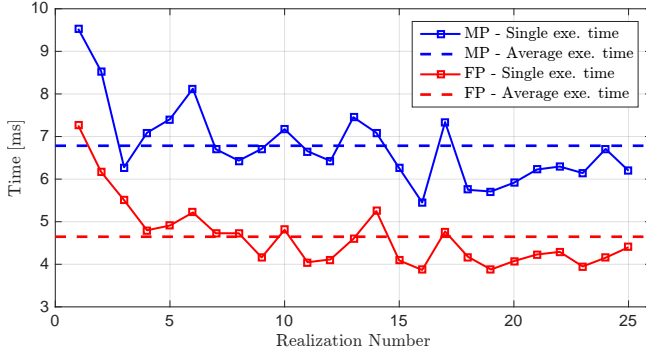
Fig. 3: Time comparison between standard MP and modified FP solvers for 25 realizations over the 118 buses transmission grid.

Matpower solver and its modified version in terms of percentage of successful realizations. The test-bed used is again the IEEE 30 buses grid. We draw 1000 Monte-Carlo samples randomizing:

- the network electrical parameters with a deviation of $\pm 5\%$ from their nominal values,
- the 50% of the demand,
- the 50% of the generation,

Table III shows how the modified FP solver behaves better or at least equal than the standard one.

MP successful realizations [%]	46.40
FP successful realizations [%]	48.30
MP and FP successful [%]	98.10
MP only successful [%]	0.00
FP only successful [%]	1.90

TABLE III: Comparison, in terms of number of successful realizations, between the standard Matpower solver and its modified FP version.

V. Conclusions

We addressed the problem of DC power flow feasibility. We built the analysis from recent results in the field. We presented a sufficient condition to ensure the existence of a solution of the power flow equations. The advantage from previous results is to take into account the effects of possible distributed generation, modeled as active/positive loads able to sustain their own load while injecting power into the grid. As a natural byproduct of reformulating the PFEs in fixed point notation, we obtained a simple yet numerically efficient algorithm to solve the PFEs. Finally, both the feasibility condition as well as the proposed algorithm have been extensively tested over standard feeders.

References

[1] J. W. Simpson-Porco, F. Dörfler, and F. Bullo, "Voltage collapse in complex power grids," *Nature Communications*, vol. 7, no. 10790, 2016.

[2] T. Van Cutsem and C. Vournas, *Voltage Stability of Electric Power Systems*. Springer, 1998.

[3] J. Machowski, J. W. Bialek, and J. R. Bumby, *Power System Dynamics*, 2nd ed. John Wiley & Sons, 2008.

[4] I. Dobson, "The irrelevance of load dynamics for the loading margin to voltage collapse and its sensitivities," in *Bulk Power System Voltage Phenomena III - Voltage Stability, Security and Control*, Davos, Switzerland, Aug. 1994.

[5] V. A. Venikov, V. A. Stroev, V. I. Idelchick, and V. I. Tarasov, "Estimation of electrical power system steady-state stability in load flow calculations," *IEEE Transactions on Power Apparatus and Systems*, vol. 94, no. 3, pp. 1034–1041, 1975.

[6] I. Dobson, "Observations on the geometry of saddle node bifurcation and voltage collapse in electrical power systems," *IEEE Transactions on Circuits and Systems I: Fundamental Theory and Applications*, vol. 39, no. 3, pp. 240–243, 1992.

[7] T. Van Cutsem, "Voltage instability: phenomena, countermeasures, and analysis methods," *Proceedings of the IEEE*, vol. 88, no. 2, pp. 208–227, 2000.

[8] T. V. Cutsem, "A method to compute reactive power margins with respect to voltage collapse," *IEEE Transactions on Power Systems*, vol. 6, no. 1, pp. 145–156, 1991.

[9] I.-L. Aolaritei, S. Bolognani, and F. Dörfler, "A distributed voltage stability margin for power distribution networks," in *IFAC World Congress [submitted]*, 2017.

[10] F. Dörfler, M. Chertkov, and F. Bullo, "Synchronization in complex oscillator networks and smart grids," *Proceedings of the National Academy of Sciences*, vol. 110, no. 6, pp. 2005–2010, 2013.

[11] B. Gentile, J. W. Simpson-Porco, F. Dörfler, S. Zampieri, and F. Bullo, "On reactive power flow and voltage stability in microgrids," in *American Control Conference*, Portland, OR, USA, Jun. 2014, pp. 759–764.

[12] S. Bolognani and S. Zampieri, "On the existence and linear approximation of the power flow solution in power distribution networks," *IEEE Transactions on Power Systems*, vol. 31, no. 1, pp. 163–172, 2016.

[13] S. Bolognani and F. Dörfler, "Fast power system analysis via implicit linearization of the power flow manifold," in *Allerton Conf. on Communications, Control and Computing*, Urbana-Champagin, IL, USA, Sep. 2015.

[14] M. Todescato, J. W. Simpson-Porco, F. Dörfler, R. Carli, and F. Bullo, "Voltage stress minimization by optimal reactive power control," *IEEE Transactions on Control of Network Systems*, Feb. 2016, submitted.

[15] A. R. Bergen and V. Vittal, *Power Systems Analysis*, 2nd ed. Prentice Hall, 2000.

[16] J. Thorp, D. Schulz, and M. Ilić-Spong, "Reactive power-voltage problem: conditions for the existence of solution and localized disturbance propagation," *International Journal of Electrical Power & Energy Systems*, vol. 8, no. 2, pp. 66–74, 1986.

[17] R. D. Zimmerman, C. E. Murillo-Sánchez, and R. J. Thomas, "MATPOWER: Steady-state operations, planning, and analysis tools for power systems research and education," *IEEE Transactions on Power Systems*, vol. 26, no. 1, pp. 12–19, 2011.

[18] T. Stuckless, "Brouwer's fixed point theorem: Methods of proof and generalizations," Ph.D. dissertation, Simon Fraser University, 2003.

The proof is split according to statements 1) and 2).

A. Proof of Statement 1)

We proceed as follows: i) we present some convenient bounds for the PFEs in fixed point notation; ii) we present necessary and sufficient conditions for the existence of the parameters δ_-^{low}, δ_+^{low}, δ_-^{up} and δ_+^{up} (equivalently for Algorithm 1 to be well-posed) and conditions to ensure the solution space to be invariant for the fixed point mapping; iii) we show contraction of the fixed point mapping.

i) First of all, from Section III-A, let us recall Eq. (12) which, defining the vector $r(x)$, x being the vector of voltage deviations from V_L^*, reads as

$$x = f(x) := -\frac{1}{4} P_{\text{crit}}^{-1} \text{diag}(P_L) r(x). \tag{13}$$

Moreover, from the definition (6) of $\overline{\mathcal{S}}(\delta)$, for any $\delta \in [0, 1[$, it follows that

$$V_L \in \overline{\mathcal{S}}(\delta) \text{ (resp. } \mathcal{S}(\delta)) \iff x \in \overline{\mathcal{B}}_\infty(\delta) \text{ (resp. } \mathcal{B}_\infty(\delta)).$$

In view of the above equivalence, in the following we work with x and $\overline{\mathcal{B}}_\infty(\delta)$ rather than V_L and $\overline{\mathcal{S}}(\delta)$. Regarding (13) as a discrete-time dynamical system, i.e., $x(k+1) = f(x(k))$, our ultimate goal is to show $\overline{\mathcal{B}}_\infty(\delta)$ is forward-invariant for the above dynamics and, in particular, that from $\mathcal{B}_\infty(\delta_+)$ the dynamics contracts until reaching $\overline{\mathcal{B}}_\infty(\delta_-)$.

Now, by splitting P_L as in (8), by considering the definition of $r(x)$ and being $x \in \overline{\mathcal{B}}_\infty(\delta)$, $f(x)$ can be upper and lower bounded by

$$f(x) \leq \frac{\|P_{\text{crit}}^{-1} P_L^+\|_{+\infty}}{4(1-\delta)} \mathbb{1} - \frac{\|P_{\text{crit}}^{-1} P_L^-\|_{-\infty}}{4(1+\delta)} \mathbb{1}, \tag{14a}$$

$$f(x) \geq \frac{\|P_{\text{crit}}^{-1} P_L^+\|_{-\infty}}{4(1+\delta)} \mathbb{1} - \frac{\|P_{\text{crit}}^{-1} P_L^-\|_{+\infty}}{4(1-\delta)} \mathbb{1}. \tag{14b}$$

Hence, given a certain δ, a simple condition for the invariance of $\overline{\mathcal{B}}_\infty(\delta)$ is to require (14a)–(14b) satisfy, respectively

$$\frac{1}{4} \frac{\|P_{\text{crit}}^{-1} P_L^+\|_{+\infty}}{1-\delta} \mathbb{1} - \frac{1}{4} \frac{\|P_{\text{crit}}^{-1} P_L^-\|_{-\infty}}{1+\delta} \mathbb{1} \leq \delta \mathbb{1}, \tag{15a}$$

$$\frac{1}{4} \frac{\|P_{\text{crit}}^{-1} P_L^+\|_{-\infty}}{1+\delta} \mathbb{1} - \frac{1}{4} \frac{\|P_{\text{crit}}^{-1} P_L^-\|_{+\infty}}{1-\delta} \mathbb{1} \geq -\delta \mathbb{1}. \tag{15b}$$

From (15a)–(15b) note that the vector $\mathbb{1}$ can be canceled out leading to two simpler scalar inequalities. Furthermore, defining $g(\delta) := 4\delta(1-\delta^2)$, rearranging the terms and exploiting the definitions in (9), we get, respectively

$$\varphi_+ + \Phi_+ \delta \leq g(\delta), \tag{16a}$$

$$\varphi_- - \Phi_- \delta \geq -g(\delta). \tag{16b}$$

Figure 4 shows an example of how these inequalities might look like.
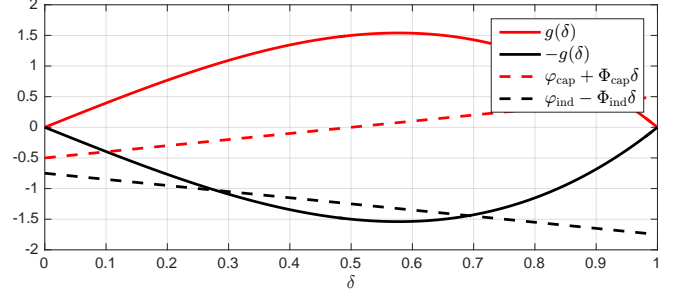
Fig. 4: Representation of the upper bound (16a) (red lines) and of the lower bound (16b) (black lines).

ii) Now, in order to prove invariance of $\overline{\mathcal{B}}_\infty(\delta)$ we first present necessary and sufficient conditions for the solvability of (16a) (resp. (16b)) and thus for the existence of $\delta_-^{\text{up}}, \delta_+^{\text{up}}$ (resp. $\delta_-^{\text{low}}, \delta_+^{\text{low}}$). Then we present a necessary and sufficient condition for the simultaneous solution of the inequalities ensuring the intersection of the two solution sets to be non-empty. We consider (16a) first.

Theorem 1.1: The following three scenarios completely characterize the solution set of (16a) for $\delta \in [0, 1]$:

1) if $\varphi_+ < 0$, solutions always exist.
2) if $0 \leq \varphi_+ \leq 1$, there exist solutions if and only if $\Phi_+ \leq 4 - 12 \left(\frac{\varphi_+}{8}\right)^{\frac{2}{3}}$;
3) otherwise no solution exists.

If 1) or 2) hold, there exist $\delta_-^{\text{up}} \in [0, \frac{1}{2}]$ and $\delta_+^{\text{up}} \in [\delta_-^{\text{up}}, 1]$ such that, for $\delta \in [\delta_-^{\text{up}}, \delta_+^{\text{up}}]$, (16a) is satisfied. $\qquad\square$

Proof: Scenario 1) is trivial. Indeed, since $\Phi_+ > 0$, if $\varphi_+ < 0$ then there exists $\epsilon > 0$ s.t. for $\delta \in [0, \epsilon[$, $y(\delta) := \varphi_+ + \Phi_+ \delta < 0$. Conversely, for all $\delta \in [0, 1]$, $g(\delta) \geq 0$. Hence, $\delta_- = 0$ while $\delta_+ \in]\delta_-, 1]$ can be computed as the solution of the third order polynomial $y(\delta) = g(\delta)$, $\delta > 0$. If the solution is ≤ 1 we set δ_+ equal to it, otherwise we set $\delta_+ = 1$.

For 2), first of all, notice that the values φ_+ and Φ_+ are not independent and such that $\varphi_+ \leq \Phi_+$. In particular, if one parameter increases the other one increases accordingly. In particular, there is one value of φ_+ beyond which the slope Φ_+ of $y(\delta)$ is such that $y(\delta) \cap g(\delta) = \emptyset$. To compute such value, we compare $y(\delta)$ and the line $y_{\text{tg}}(\overline{\delta}, \delta) := s(\overline{\delta})\delta + i(\overline{\delta})$ tangent to $g(\delta)$ at $\overline{\delta}$. Indeed, solutions exist only if $y \leq y_{\text{tg}}$ point-wise. The functions $s(\overline{\delta})$ and $i(\overline{\delta})$ identify slope and intercept of $y_{\text{tg}}(\overline{\delta}, \delta)$ and are equal to, respectively

$$s(\overline{\delta}) = 4 - 12\overline{\delta}^2; \qquad i(\overline{\delta}) = 8\overline{\delta}^3; \qquad \overline{\delta} \in \left[0, 1/\sqrt{3}\right[.$$

Their values define the set of tangent lines to $g(\delta)$; see Figure 5. Note that at $\overline{\delta} = 1/\sqrt{3}$, $g(\delta)$ attains its maximum hence, after that point $s(\overline{\delta}) < 0$ and the comparison between y and y_{tg} is meaningless. Now, imposing $\varphi_+ = i(\overline{\delta})$ and solving for $\overline{\delta}$, one obtain $\overline{\delta} = \left(\frac{\varphi_+}{8}\right)^{\frac{1}{3}}$. This identifies a particular tangent line $y_{\text{tg}}(\overline{\delta}, \delta)$,
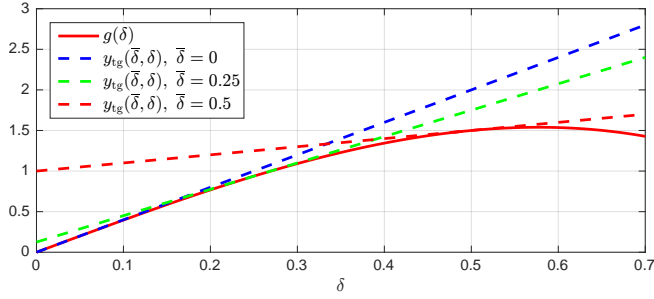
Fig. 5: Line $y_{\text{tg}}(\delta)$ tangent to $g(\delta)$ for different values of $\bar{\delta}$.

whose slope is equal to

$$s(\bar{\delta}) = 4 - 12\left(\frac{\varphi_+}{8}\right)^{\frac{2}{3}},$$

and it is easy to understand that $y(\delta)$ intersects $g(\delta)$ in at least one point if and only if its slope Φ_+ satisfies

$$\Phi_+ \le 4 - 12\left(\frac{\varphi_+}{8}\right)^{\frac{2}{3}},$$

that is, if and only if y is not above y_{tg}. In particular, if $y(\delta) < y_{\text{tg}}(\bar{\delta}, \delta)$, for $\delta > 0$, then it intersects $g(\delta)$ in two points, $\delta_-^{\text{up}} \in [0, 1/\sqrt{3}[$ and $\delta_+^{\text{up}} \in]\delta_-^{\text{up}}, 1]$; conversely, if $y(\delta) = y_{\text{tg}}(\bar{\delta}, \delta)$ point-wise then, for the equation $y(\delta) = g(\delta)$ there exist two solutions $\delta_-^{\text{up}}, \delta_+^{\text{up}}$ s.t. $\delta_-^{\text{up}} = \delta_+^{\text{up}} = \bar{\delta} \in [0, 1/\sqrt{3}[$.
Regarding 3) we must show that for $\varphi_+ > 1$ no solution exists. Recall that $1 < \varphi_+ \le \Phi_+$. However, $i(\bar{\delta}) = 1$ corresponds to $\bar{\delta} = 1/2$ and thus to $s(\bar{\delta}) = 1 < \Phi_+$, meaning that $y(\delta) > y_{\text{tg}}(\bar{\delta}, \delta)$, for $\delta \ge 0$. Thus no intersection exists.
Finally, we show that $\delta_-^{\text{up}} \in [0, 1/2]$. Indeed, assume $\bar{\delta} > 1/2$. Then, $i(\bar{\delta}) > s(\bar{\delta})$ which is against $\varphi_+ \le \Phi_+$ and thus $y(\delta) > y_{\text{tg}}(\bar{\delta}, \delta)$. This means that, for cases 1) and 2), it actually holds $\delta_-^{\text{up}} \in [0, 1/2]$. ∎

Remark 1.2: Observe that, even if the limit value $\varphi_+ = 1$ is admissible in practice, this is never achieved in the case of mixed loads. This is because, thanks to Theorem 1.1, there exists a solution if and only if

$$\varphi_+ = \Phi_+ = 1.$$

This is equivalent to

$$1 = \|P_{\text{crit}}^{-1} P_L^+\|_{+\infty} - \|P_{\text{crit}}^{-1} P_L^-\|_{-\infty}$$
$$= \|P_{\text{crit}}^{-1} P_L^+\|_{+\infty} + \|P_{\text{crit}}^{-1} P_L^-\|_{-\infty}$$

which is achieved only if $\|P_{\text{crit}}^{-1} P_L^-\|_{-\infty} = 0$ and so $\|P_{\text{crit}}^{-1} P_L^+\|_{+\infty} = 1$. This is an admissible scenario but it is not of particular interest since we want to analyze the interaction between the positive and negative part of the load. ∎

Regarding (16b), for symmetry of the inequalities, a similar theorem can be stated.

Theorem 1.3: The following three scenarios completely characterized the solution set of (16b) for $\delta \in [0, 1]$:

1) if $0 < \varphi_-$, solutions always exist.
2) if $-1 \le \varphi_- \le 0$, there exist solutions if and only if
$$\Phi_- \le 4 - 12\left(-\frac{\varphi_-}{8}\right)^{\frac{2}{3}};$$
3) otherwise no solution exists.

If 1) or 2) hold, exist $\delta_-^{\text{low}} \in [0, \frac{1}{2}]$ and $\delta_+^{\text{low}} \in [\delta_-^{\text{low}}, 1]$ such that, for $\delta \in [\delta_-^{\text{low}}, \delta_+^{\text{low}}]$, (16b) is satisfied. ∎

Theorems 1.1 and 1.3 give necessary and sufficient conditions for the existence of solutions of (16a) and (16b), respectively. However, their simultaneous solution is still not sufficient for the invariance of $\overline{\mathcal{B}}_\infty(\delta)$ and indeed, it is necessary to verify the intersection of their solution sets is non empty. The following theorem can be easily verified by graphical inspection.

Theorem 1.4: Assume that both (16a) and (16b) have non empty solutions sets and define $\delta_- := \max\{\delta_-^{\text{low}}, \delta_-^{\text{up}}\}$ and $\delta_+ := \min\{\delta_+^{\text{low}}, \delta_+^{\text{up}}\}$. Then

$$\mathcal{D} := \Big\{\delta \in [\delta_-, \delta_+] \mid \varphi_+ + \Phi_+\delta \le g(\delta) \ \text{and}$$
$$\varphi_- - \Phi_-\delta \ge -g(\delta)\Big\} \ne \emptyset$$

if and only if $\delta_-^{\text{up}} < \delta_+^{\text{low}}$ and $\delta_-^{\text{low}} < \delta_+^{\text{up}}$. ∎

iii) To conclude we need to prove existence of a solution inside $\overline{\mathcal{S}}(\delta_-)$ only, indeed, so far, thanks to *Brouwer's fixed point theorem* [18], it is possible to conclude existence of a solution in any $\overline{\mathcal{S}}(\delta), \delta \in [\delta_-, \delta_+]$. Let us regard Eq. (13) as the equilibrium of the discrete-time dynamical system $x(k+1) = f(x(k))$ and assume $x(k) \in \mathcal{B}_\infty(\delta_+)$. Then, there exists $x(k) \in \mathcal{B}_\infty(\delta), \delta < \delta_+$ such that $\|x(k)\|_\infty = \delta$. From the results above we have that

$$-\delta\mathbb{1} \le f(x) \le \delta\mathbb{1} \quad \text{if} \ \delta \in [\delta_-, \delta_+],$$
$$-\delta\mathbb{1} < f(x) < \delta\mathbb{1} \quad \text{if} \ \delta \in]\delta_-, \delta_+[,$$

meaning that $\|f(x)\|_\infty < \delta$ for $\delta \in]\delta_-, \delta_+[$. Hence

$$\|x(k+1)\|_\infty = \|f(x(t))\|_\infty < \|x\|_\infty = \delta, \quad \delta \in]\delta_-, \delta_+[.$$

This reasoning can be propagated at the successive iteration eventually contracting until we hit $\|x(\bar{k})\|_\infty = \delta_-$ for some $\bar{k} > k$. This means that starting from $\overline{\mathcal{B}}_\infty(\delta)$ for $\delta \in [\delta_-, \delta_+[$, our forward invariant set $\overline{\mathcal{B}}_\infty(\delta)$ shrinks, reaching $\overline{\mathcal{B}}_\infty(\delta_-), \delta_- \in [0, \frac{1}{2}]$. Finally, it automatically follows from the contraction argument the absence of solutions inside $\mathcal{S}(\delta_+) \setminus \overline{\mathcal{S}}(\delta_-)$.

B. Proof of Statement 2)

Notice that in the interval $]-\delta_+, +\infty[$, each component of $r(x)$, i.e., $r_i(x_i) = 1/(1 + x_i)$ is strictly monotone and $\|r(k)\|_\infty < 1/(1 - \delta_+)$. Thus, given $x(k) \in]-\delta_+, +\infty[^n$ it follows that (14a)–(14b) are strict and, in turn, $\|x(k+1)\|_\infty = \|f(x(k))\|_\infty < \delta_+$. Hence $x(k+1) \in \mathcal{B}_\infty(\delta_+)$. Together with the contraction argument above, Statement 2) follows.